V International Conference on Particle-based Methods – Fundamentals and Applications
PARTICLES 2017
P. Wriggers, M. Bischoff, E. Oñate, D.R.J. Owen, & T. Zohdi (Eds)

MODELLING OF CHEMICAL REACTIONS IN METALLURGICAL PROCESSES

MUSTAFA E. KINACI[1], THOMAS LICHTENEGGER[2,3] AND SIMON SCHNEIDERBAUER[1,3]

[1] Christian Doppler Laboratory for Multi-Scale Modelling of Multiphase Processes
4040 Linz, Austria
mustafa_efe.kinaci@jku.at

[2] Linz Institute of Technology (LIT), Johannes Kepler University
4040 Linz, Austria
thomas.lichtenegger@jku.at

[3] Department of Particulate Flow Modelling, Johannes Kepler University
4040 Linz, Austria
simon.schneiderbauer@jku.at

Key words: CFD-DEM, Iron-ore reduction, Chemical models, Particle shrinkage, Unreacted-core model, Diffusion coefficients

Abstract. Since the last three decades, the study of reduction of iron-ore has gained much attention as it is considered a core process for the steel industry. Fluidized bed and moving bed reactors are utilized to reduce the iron-ore efficiently. As reducing agents coal, coke or natural gases are used, which are released as CO_2 gas, or sometimes in small amounts as H_2O to the environment. The conditions in these reactors are harsh and provide limited accessibility, therefore computational tools are used to investigate them. One such tool is the CFD-DEM method, where the reacting gas species and the governing equations for the gas flow are calculated in the Eulerian (CFD) side, whereas the particle reactions and equation of motion are calculated in the Lagrangian (DEM) side.

In the current work, the CFD-DEM method is extended to cover the most dominant types of models for heterogeneous reactions between submerged solids and fluids. One of these models is the Shrinking Particle Model (SPM), which is used to verify the communication framework between the CFD and DEM sides by running preliminary test cases. Another model is the Unreacted Shrinking Core Model (USCM), which is considered as a good model for a reality like iron-ore reduction modelling.

1 INTRODUCTION

The deterioration of the quality of ore and coal due to high costs and low availability related with the shortage of resources has led to increase in research of iron ore reduction. The practical importance of being used as a feedstock for steel-making processes has also played an important role [1, 2].

The leading process used in iron-making is the blast furnace. These furnaces consists of a moving bed reactor with countercurrent flow of the solid reactants against a reducing gas. In the blast furnace process, the iron ore fines which built up around 80% of iron ores, need to go through a pelletizing or sintering process [3]. In some cases, such as the fluidized bed technology, fine ores can directly be charged into the reduction process making it highly advantageous. Such fluidized bed reactors are used in the pre-reduction stage of the FINEX® process [4, 5]. The FINEX® process, which was jointly developed by POSCO (Korea) and Primetals Technologies (Austria), produces hot metal in the same quality as traditional blast furnaces, without the need for sintering and coke making. The iron-ores that are charged into the process go through fluidized bed reactors where they are heated and reduced to Direct Reduced Iron (DRI). The DRI is then charged into the melter gasifier where the final reduction and melting as well as the production of reducing gas by gasification of coal with oxygen takes place. Another advantage of the FINEX® process is the exhaust gas, which can be used for various other applications such as heating within a steel plant, power generation and so forth [6].

The main reactions for the reduction of metallic oxide with a gaseous reductant (CO or H_2) can be expressed with the following reaction steps:

$$3\,Fe_2O_3 + CO/H_2 \longrightarrow 2\,Fe_3O_4 + CO_2/H_2O \tag{1}$$

$$Fe_3O_4 + CO/H_2 \longrightarrow 3\,FeO + CO_2/H_2O \tag{2}$$

$$FeO + CO/H_2 \longrightarrow Fe + CO_2/H_2O \tag{3}$$

The conditions inside the reactors limit accessibility thereby complicating the physical investigation of the processes. Thus, simulation methods and computational tools are used to improve the iron-making processes. One such tool is the Two-Fluid Model (TFM), which is an Euler-Euler approach that treats the solid and the fluid phases as a continuum. However, this model lacks the proper representation of particle size description and the related physical phenomena. In order to represent micro-scale phenomena, the TFM would require a fine spatial grid, which would make the computation unaffordable for industrial scale utilization. If coarse-graining is carried out there would be a loss of unresolved (small) scales and might lead to errors [8, 7]. Another tool uses the coupling of Computational Fluid Dynamics (CFD) for the continuous fluid phase (i.e. the reduction gas) and the Discrete Element Method (DEM) for the discrete particles

such as iron-ore and coal. These methods are coupled in a CFD-DEM approach based on the open source software packages OpenFOAM (OpenCFD Ltd. 2009) and LIGGGHTS (LIGGGHTS, 2011) [9]. DEM provides an easier way to evaluate the per-particle chemistry such as the shrink/growth of particles due to reactions and it does not require to transfer these reactions to a continuum representation. However, to tackle industrial scale operations with the CFD-DEM, coarse-graining needs to be carried out in order to reduce the computational demands. Another method that can be thought of would be the hybrid Lagrangian-Eulerian model that combines the Lagrangian Discrete Phase Model (DPM) and a coarse-grained TFM such as in the works of Schneiderbauer et al. [10].

2 REACTION KINETICS

The most common types of representation models for the non-catalytic reactions of solids submerged in fluids are the shrinking particle model (SPM) and the unreacted shrinking core model (USCM) [11]. In the SPM, only the surface of the particle reacts with the surrounding fluid therefore there is no layer formation due to the reaction and the products diffuse directly into gas. As the reaction progresses, the particle shrinks and eventually disappears completely. In the USCM, as the particle surface reacts and shrinks it forms a layer behind. The reductant gas has to diffuse through this layer in order to react with the core.

The main reactions for the direct reduction of iron with a gaseous reductant, CO/H_2, can be expressed in three reaction steps as shown in reaction equations 1 - 3. The three layer USCM developed by Philbrook, Spitzer and Manning [12] is able to represent the three interfaces of hematite/magnetite, magnetite/wustite and wustite/iron adequately. The reduction of iron-oxide to produce metallic iron follows these steps [12];

- The reducing gas is transported through the gas film onto the particle surface.
- The reductant gas then diffuses through the porous iron layer.
- Part of the reductant reacts with wustite at the wustite/iron interface producing iron and gaseous product.
- Rest of the reducing gas diffuses through the wustite layer onto the wustite/magnetite interface.
- A portion of the gas reacts with magnetite at layer surface producing wustite and gaseous product.
- The balance gas diffuses through the magnetite layer onto the magnetite/hematite interface.
- Chemical reaction of the leftover gas occurs at the hematite core and produces magnetite and a gaseous product.

- The gaseous product diffuses outwards through the pores of the pellet.

Since each step poses a resistance to the total reduction of the pellet, the reduction pattern of a single pellet can be considered to follow a resistance network such as an electrical resistance circuit network as illustrated in Fig. 1.

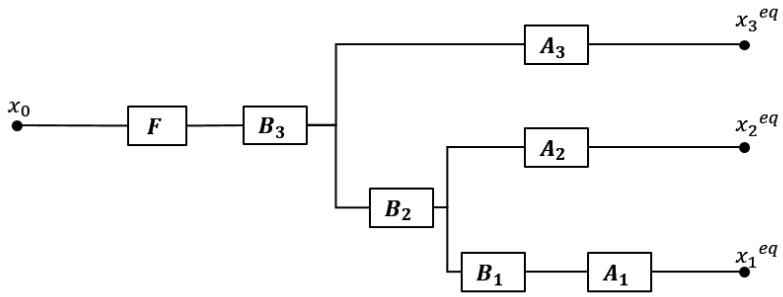

Figure 1: Resistance network diagram that illustrates the resistance of an iron-ore pellet that goes through in the reduction process.

The solution of the resistance network yields the reaction flow rate $\dot{Y}_{i,j}$ for every layer that can be defined as

- from hematite to magnetite

$$\begin{aligned}\dot{Y}_{i,h} = [([A_3(A_2+B_2+B_3+F)+(A_2+B_2)(B_3+F)](x_0 - x^{eq}_{CO,1}) \\ - [A_3(B_2+B_3+F)+B_2(B_3+F)](x_0 - x^{eq}_{CO,2}) \\ - [A_2(B_3+F)](x_0 - x^{eq}_{CO,3}))\frac{1}{W}]_i\end{aligned} \tag{4}$$

- from magnetite to wustite

$$\begin{aligned}\dot{Y}_{i,m} = [([(A_1+B_1+B_2)(A_3+B_3+F)+A_3(B_3+F)](x_0 - x^{eq}_{CO,2}) \\ - [B_2(A_3+B_3+F)+A_3(B_3+F)](x_0 - x^{eq}_{CO,1}) \\ - [(A_1+B_1)(B_3+F)](x_0 - x^{eq}_{CO,3}))\frac{1}{W}]_i\end{aligned} \tag{5}$$

- from wustite to iron

$$\begin{aligned}\dot{Y}_{i,w} = [([(A_1+B_1)(A_2+B_2+B_3+F)+A_2(B_2+B_3+F)] \\ (x_0 - x^{eq}_{CO,3}) - [A_2(B_3+F)](x_0 - x^{eq}_{CO,1}) \\ - [(A_1+B_1)(B_3+F)](x_0 - x^{eq}_{CO,2}))\frac{1}{W}]_i\end{aligned} \tag{6}$$

in which $A_{i,j}$ represents the relative chemical reaction resistance term, $B_{i,j}$ the relative diffusivity resistance term, j represents the layers hematite, magnetite and wustite and i the reducing gas species. F is the mass transfer resistance term, which is defined with $1/k_f$. x_0 is the bulk gas mole fraction and $x_{i,j}^{eq}$ the relative layer equilibrium mole fractions. The denominator W is expressed as

$$\begin{aligned} W = &[(A_1 + B_1)(A_3(A_2 + B_2 + B_3 + F) + (A_2 + B_2)(B_3 + F)) \\ &+ A_2(A_3(B_2 + B_3 + F) + B_2(B_3 + F))]_i \end{aligned} \tag{7}$$

The equilibrium mole fractions of the reducing gas species can be defined with the equilibrium constant. The equilibrium constant Keq_j, is the ratio of product to reactant equilibrium mole fractions, and represented as

$$\frac{x_{prod,j}^{eq}}{x_{reac,j}^{eq}} = Keq_{\mathrm{Fe_xO_y,CO}}. \tag{8}$$

With the help of the reaction flow rate $\dot{Y_{i,j}}$, the reactant gas mass change for every layer is calculated as

$$\frac{dm_{i,j}}{dt} = \dot{Y}_{i,j}\rho_g 4\pi r^2, \tag{9}$$

where i is the reactant gas species such as CO or H_2, ρ_g is the gas density, r is the particle radius. With the help of the reactant gas mass change, one is able to calculate the mass change of every layer and the product gas as

$$\frac{dm_{k,j}}{dt} = \frac{dm_{i,j}}{dt}\frac{\upsilon_k}{\upsilon_j}\frac{M_k}{M_j}, \tag{10}$$

in which k is either the layer species of the iron-ore pellet Fe_2O_3, Fe_3O_4, FeO, Fe or the product gas of H_2O or CO_2. The υ is the stoichiometric coefficient of the relative species, and M is the molar mass of relative species.

The chemical reaction resistance term $A_{i,j}$ can be expressed as

$$A_{i,j} = \left[\frac{1}{(1-f_j)^{\frac{2}{3}}}\frac{1}{k_j\left(1-\frac{1}{Keq_j}\right)}\right]_i \tag{11}$$

in which j represents the reduction layer, i the reducing gas,. k_j is the reaction rate constant for layer j and is determined as

$$k_j = k_0 \exp(\frac{-E_a}{RT}), \tag{12}$$

the values for the pre-exponential factor k_0, and the activation energy E_a can be found in literature[13]. f_j is the local fractional reduction of the relative layer that is calculated as

$$f_j = 1 - \left(\frac{r_j}{r_p}\right)^3. \tag{13}$$

The diffusivity resistance term $B_{i,j}$ can be calculated for the relative iron oxide component as [13]

$$B_{i,h} = \left[\frac{(1-f_m)^{\frac{1}{3}} - (1-f_h)^{\frac{1}{3}}}{(1-f_m)^{\frac{1}{3}}(1-f_h)^{\frac{1}{3}}} \frac{r_g}{D_h^{eff}}\right]_i, \tag{14}$$

$$B_{i,m} = \left[\frac{(1-f_w)^{\frac{1}{3}} - (1-f_m)^{\frac{1}{3}}}{(1-f_w)^{\frac{1}{3}}(1-f_m)^{\frac{1}{3}}} \frac{r_g}{D_m^{eff}}\right]_i, \tag{15}$$

$$B_{i,w} = \left[\frac{1-(1-f_w)^{\frac{1}{3}}}{(1-f_w)^{\frac{1}{3}}} \frac{r_g}{D_w^{eff}}\right]_i, \tag{16}$$

in which D_j^{eff} represents the effective diffusion coefficient of the relative layer.

2.1 Diffusion Coefficients

The diffusion of a gas through a porous medium, in this case the porous iron-ore pellet, depends on the molecular and Knudsen diffusions. If the Knudsen number, the ratio of the mean free path of the gas molecules to the pore diameter, is smaller than 0.1 molecular diffusion becomes predominant. If the Knudsen number is larger than 10, then Knudsen diffusion becomes prevalent [14, 15].

The Knudsen diffusion for diffusing species i, $D_{i,K}$ can be determined with [14, 15, 16]

$$D_{i,K} = \frac{\phi_{pore}}{3}\sqrt{\frac{8k_BNT}{\pi M_i}}. \tag{17}$$

where $k_B = 1.38066 \times 10^{-16 g \cdot cm/s^2 K}$ is the Boltzmann constant, and $N = 6.023 \times 10^2 3^{molecules/mol}$ is the Avogadro's constant, ϕ_{pore} is the pore diameter and M_i represents the molar mass of species i.

The effective Knudsen diffusion can be defined as a function of porosity, ε , and tortuosity, τ for layer j of the iron-ore particle with

$$D_{j,K}^{eff} = \frac{\varepsilon_j}{\tau_j} D_{i,K} \tag{18}$$

There are various diffusion coefficient correlations for binary molecular diffusion. The most common method is the *Chapman-Enskog* correlation, which is derived from the particle collision diameters and the Lennard-Jones potentials. Since for some gases the estimates for collision diameters or Lennard-Jones parameters are not available [14, 17], other empirical correlations have been proposed. A slightly better correlation

$$D_{i,j} = \frac{10^{-3} T^{1.75} \left(\frac{1}{M_i} + \frac{1}{M_j}\right)^{(1/2)}}{p \left[\left(\sum_i \nu_i\right)^{(1/3)} + \sum_j \nu_j^{(1/3)}\right]^2} \tag{19}$$

where M is the relative gas molar mass, and ν the diffusion volume of the specified species has been proposed by Fuller, Schettler and Giddings [16, 17]. The values for the diffusion volumes are defined in Table 1.

Table 1: Diffusion volumes for various species [17]

Atomic and Structural Diffusion Volume Increments			
C	16.5	H	1.98
O	5.48	N	5.69
Diffusion Volume of Simple Molecules			
H_2	7.07	N_2	17.9
O_2	16.6	Air	20.1
CO	18.9	CO_2	26.9
N_2O	35.9	H_2O	12.7

The diffusion coefficient in multicomponent mixtures is then calculated as [18, 19]

$$D_{i,m} = (1 - x_i) \left(\sum_{i \neq j} \frac{x_j}{D_{i,j}}\right)^{-1}, \tag{20}$$

in which x is the mole fraction. Just like the effective Knudsen diffusion coefficient, the effective diffusion coefficient for multicomponent mixtures is determined by multiplying the diffusion term with the ratio of porosity to tortuosity as

$$D_{j,m}^{eff} = \frac{\varepsilon_j}{\tau_j} D_{i,m}. \tag{21}$$

The total effective diffusion can thus be defined as

$$\frac{1}{D_j^{eff}} = \frac{1}{D_{j,m}^{eff}} + \frac{1}{D_{j,K}^{eff}}. \tag{22}$$

3 RESULTS

The CFD-DEM coupling library is extended to cover the SPM. This model is used to verify if the communication framework between the Eulerian and the Lagrangian sides. The communication of DEM and CFD works by first initializing the particles on the DEM side and transferring their information such as the locations and velocities to the CFD

side. This information is then used to localize the particles and determine the voidfraction, fluid density, temperature, drag force and the species concentration (mass fractions) at particle locations. These data are communicated back to the DEM side. The newly transferred data is then used to determine the particle movement, the change in particle size and change of gas concentrations for the new time step. After DEM calculations, the new data is transferred back to CFD side. This process continues until a specified amount of time steps have been computed.

A simple test case is developed, consisting of a single carbon particle that reacts with the reactant gas of O_2 with a user defined reaction rate constant. The test case results are verified by comparing the species mass balances. The particle reacts only with the O_2 present, and stops after the total amount of O_2 has been depleted. The mass change of the reactant and product gas species is investigated in relation to particle shrinking. The simulation results are compared with theoretical data that is calculated with the same species concentration as the simulation, which prove to be in a good agreement. The mass change of the gas species is illustrated depending on the time in Fig. 2.

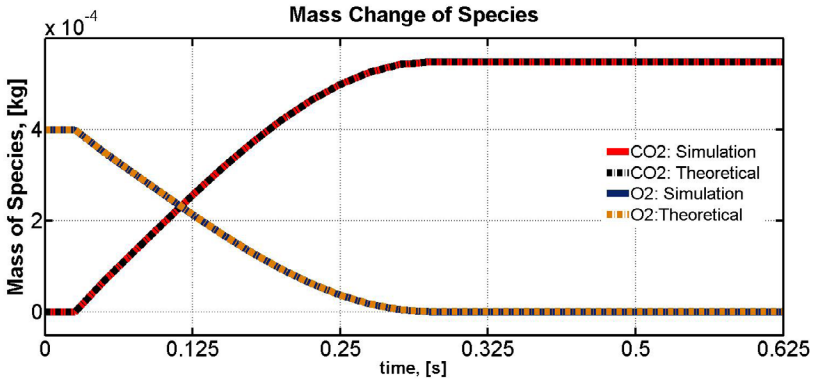

Figure 2: The change of mass of reacting gas species O_2 and product gas CO_2 depending on time.

After the communication framework has successfully been established, the USCM is implemented. At first, only the reaction resistance terms A_j is considered. An iron-ore pellet with diameter of 0.2 dm is placed in a rectangular domain with a volume of 375 m^3 and a cell volume of 1.80 m^3. The relative radii for hematite, magnetite and wustite layers are set to $0.3, 0.5$ and 0.6 respectively. The reactant gas CO reacts with the particle to produce CO_2. The fractional reduction of the relative layers with only the reaction resistance term is illustrated in Fig. 3a, and the shrinking of radii is illustrated in Fig. 3b.

The simulation is run for 3 seconds, however as the fluid velocity is practically zero, to make the reduction process faster the mass changes of the reactant gas, the pellet layer, and product gas are increased numerically with 10^4. As there is no flow, the Eulerian side is not affected by this scale up. As, the reduction of the layers with only the reaction

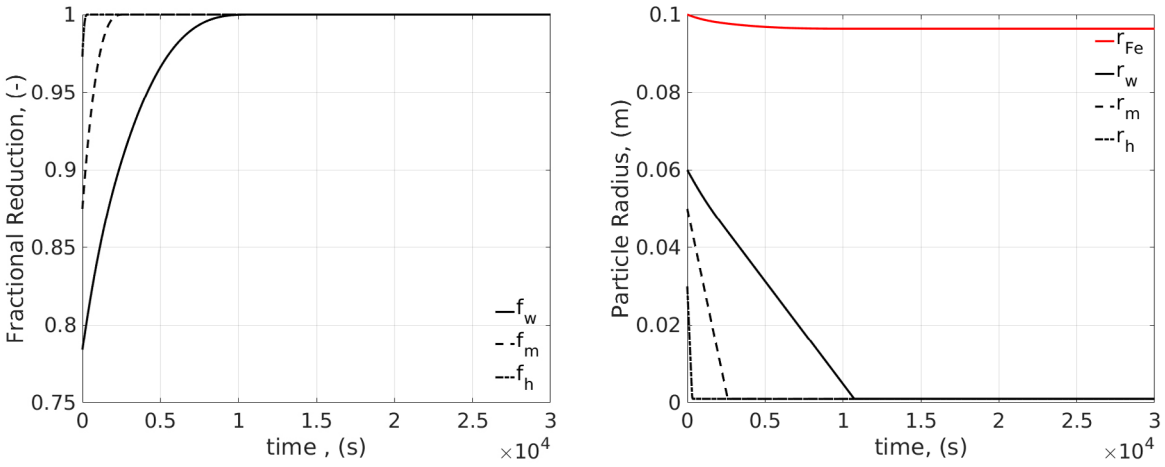

(a) The fractional reduction.

(b) The layer radii shrink.

Figure 3: The reduction of an iron-ore pellet with only the reactions resistance term.

resistance term proved successful results, the previously defined diffusion coefficient of FSG, Knudsen diffusion and the effective total diffusion coefficient is also added to the model. The particle properties that have been defined for the test case are defined in Table 2.

Table 2: The particle properties used in test case.

Parameter	Symbol	Value	Unit
Porosity	ϵ_p	15	%
Tortuosity	τ_p	3	(-)
Pore Diameter	d_p	3.61×10^{-9}	m

It is clear that the time of layer reduction increases drastically with the activation of the diffusion coefficient resistance term. With the same amount of upscaling not even the hematite core is reduced as illustrated in Fig. 4a. An upscaling of 10^8 is carried out, to see the total fractional reduction with the diffusion resistance term. It can be seen that the particle totally reduces first when at 2.7×10^8 seconds real time as illustrated in Fig. 4b.

4 CONCLUSION AND OUTLOOK

The mathematical models representing the fluid-solid chemical reactions have been implemented into the DEM library, so that the CFD-DEM method can be used to investigate the reduction of iron-ore inside the fluidized bed reactors. First, the SPM has been

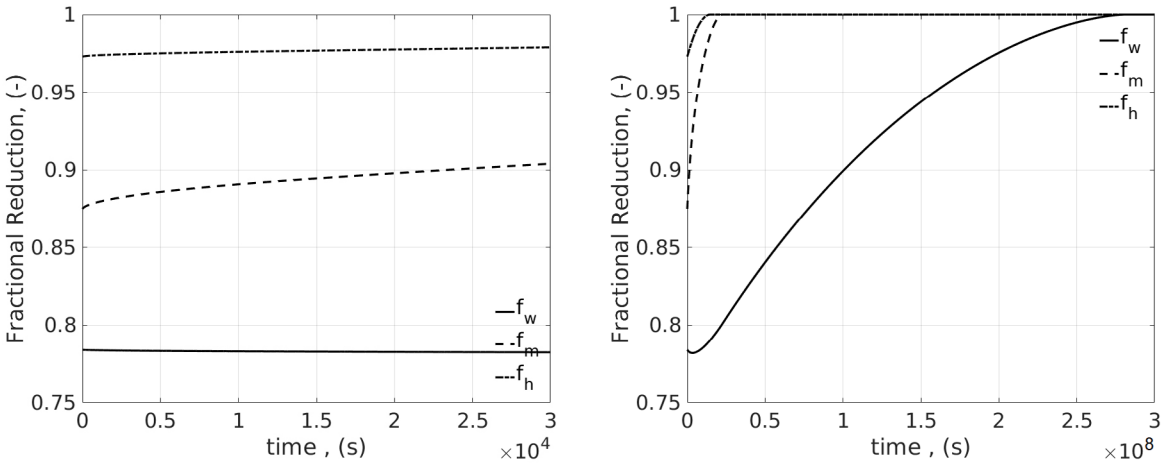

(a) Scale up of 10^4. (b) Scale up of 10^8.

Figure 4: The fractional reduction of an iron-ore pellet with the diffusion resistance term and various scale up factors.

implemented and verified. A test case is constructed to check the communication framework between CFD and DEM sides. As the communication was successfully established, the framework was expanded to cover the three-layered USCM. The USCM is considered as a valid model to represent the reduction of iron-ore. Simulations have been carried out that considered only the reaction resistance terms. It has been seen that the particle layers reduce in a reasonable manner. Afterwards, the diffusion resistance term has been added to the equations. With the addition of the diffusion resistance term, the time it took for the layers to shrink increased greatly.

Further research involves implementing the mass transfer coefficient to the coupling library, considering the effects of different pore diameters, particle porosities and tortuosities. After a thorough investigation and comparison with literature, a coarse-graining of the CFD-DEM approach will be carried out and even maybe a combination of the TFM and DPM for industrial scale simulations.

REFERENCES

[1] Donskoi, E., and McElwain, D. L. Estimation and modeling of parameters for direct reduction in iron ore/coal composites: Part I. Physical parameters. *Metallurgical and Materials Transactions B.* **34(1)**:93–102. (2003).

[2] Turkdogan, E. T., and R. J. Fruehan. Fundamentals of iron and steelmaking. *The Making, Shaping and Treating of Steel, Steelmaking and Refining Volume, 11th ed., RJ Fruehan, ed., AISE Steel Foundation, Pittsburgh* **11**:125–126.

[3] Schenk , J. L. Recent status of fluidized bed technologies for producing iron input materials for steelmaking. *Particuology.* **9(1)**:14–23. (2011).

[4] Habermann, A., Winter, F., Hofbauer, H., Zirngast, J., and Schenk, J. L. An experimental study on the kinetics of fluidized bed iron ore reduction. *ISIJ international* **40**:935–942.

[5] POSCO and Primetals Technologies. *The FINEX Process.* (2015).

[6] Plaul, F. J., C. Bhm, and J. L. Schenk. Fluidized-bed technology for the production of iron products for steelmaking. *Journal of the Southern African Institute of Mining and Metallurgy* **109.2**:121–128. (2009).

[7] Schneiderbauer, S. and Pirker, S. Filtered and Heterogeneity-Based Subgrid Modifications for Gas-Solid Drag and Solid Stresses in Bubbling Fluidized Beds. *American Institute of Chemical Engineers.* **3**: 839–854. (2014).

[8] van der Hoef, M. A. et al. Multiscale Modeling of Gas-Fluidized Beds. *Advances in Chemical Engineering* **31**:65–149. (2006).

[9] Goniva, C., et al. Influence of rolling friction on single spout fluidized bed simulation. *Particuology.* **10**:582–591. (2012)

[10] Schneiderbauer, S. et al. A Lagrangian-Eulerian Hybrid Model for the Simulation of Poly-disperse Fluidized Beds: Application to Industrial-scale Olefin Polymerization. *submitted to Powder Technology.* (2016).

[11] Levenspiel, O. *Chemical Reaction Engineering.* Oregon State University Book Stores, Inc. (1989).

[12] Tsay, Q. T., Ray, W. H. and Szekley, J. The modeling of hematite reduction with hydrogen plus carbon monoxide mixture. *AIChE J* **22**:1064–1076. (1976).

[13] Valipour, M.S. and Hashemi,M.Y. Motamed and Saboohi, Y. Mathematical modeling of the reaction in an iron ore pellet using a mixture of hydrogen, water vapor, carbon monoxide and carbon dioxide: an isothermal study. *Advanced Powder Technology* (2006) **17**:277–295.

[14] Cussler, E.L. *Diffusion: mass transfer in fluid systems*. Cambridge University Press. (2009).

[15] He, W. Lv, W. and Dickerson, J. *Gas Transport in Solid Oxide Fuel Cells*. Springer. (2014).

[16] Welty, J. R., Wicks, C. E., Rorrer, G. and Wilson, R. E. *Fundamentals of Momentum, Heat, and Mass Transfer*. John Wiley & Sons. (2009).

[17] Fuller, E. N., Schettler, P. D. and Giddings, J. C. A new method for prediction of binary gas-phase diffusion coefficients.*Industrial and Engineering Chemistry* (1966) **16**: 18-27.

[18] Elnashaie, S. S. *Modelling, simulation and optimization of industrial fixed bed catalytic reactors*. Vol. 7. CRC Press, 1994.

[19] Wilke, C. R., and Pin, C. Correlation of diffusion coefficients in dilute solutions. *AIChE Journal* (1955) **1**:264–270.